



Contents lists available at ScienceDirect

## Arabian Journal of Chemistry

journal homepage: [www.ksu.edu.sa](http://www.ksu.edu.sa)

# Biological evaluation of sophoridine by interaction with plasma transport protein and protective effects in cardiomyocytes

Zheng Wu, Shujuan Cheng, Shaoping Wang, Wenzheng Li, Jinghua Liu\*

Department of 28 Division of Cardiovascular, Beijing Anzhen Hospital, Capital Medical University, Beijing Institute of Heart, Lung and Blood Vessel Diseases, Beijing 100029, China

## ARTICLE INFO

**Keywords:**  
Sophoridine  
Alpha-2-macroglobulin  
Cardioprotective effect

## ABSTRACT

Numerous studies have demonstrated the protective benefits of sophoridine, a bioactive alkaloid, on cell damage. However, its primary biological properties such as interaction with plasma protein, which serves as the primary drug carrier, and its cardioprotective properties are still unknown. In the present study, we aimed to analyze the binding characteristics of sophoridine with alpha-2-macroglobulin ( $\alpha 2M$ ) by spectroscopic and theoretical studies. Then, the cardioprotective effects of sophoridine on myocardial ischemia/reperfusion (MI/R) injury *in vitro* were investigated using H9c2 cardiomyocytes. The results reveal that one molecule of sophoridine favorably binds to one molecule of  $\alpha 2M$  dominantly through interaction with hydrophobic amino acid residues (VAL758, PHE735, PHE735, and TRP739). Also, sophoridine leads to partial changes in the structure of this carrier protein in the vicinity of TRP739 residue. Cellular assays exhibit that sophoridine recovered cell viability, membrane leakage, and apoptosis induced by MI/R injury. It was detected that sophoridine could mitigate the oxidative stress and intrinsic apoptosis pathway through regulation of Bax, Bcl-2, and caspase. ELISA analysis also exhibits that sophoridine upregulates phosphorylation of Akt and PI3K in H9c2 cells. Our findings suggest that sophoridine could show favorable plasma protein interaction and promising cardioprotection against MI/R injury mediated by the upregulation of PI3K/AKT signaling pathway.

## 1. Introduction

Alkaloids are a significant group of bioactive compounds found in plants that show potent protective effects against oxidative stress and cell death (Shi et al., 2014; Macáková et al., 2019). One class of alkaloids with potent pharmacological significance is quinazolines (Alagarsamy et al., 2018). The quinolizidine-based alkaloid sophoridine, referred to 5 $\beta$ -Matrine, found in numerous traditional Chinese herbs including *Sophora alopecuroides* L, *Euchresta japonica* Benth, and *Sophora moorcroftiana* (Wang et al., 2022) has shown promising pharmacological activities (Chen et al., 2023; Tang et al., 2023).

Numerous investigations have verified sophoridine's anti-tumor (ur Rashid et al., 2020), anti-arrhythmia (Song et al., 2023), anti-arthritis (Song et al., 2023), and anti-inflammatory properties (Dong et al., 2022) in addition to its antioxidant activity (Dong et al., 2022). These pharmacological characteristics might indicate that sophoridine could be useful in the management and prevention of a wide range of illnesses, especially myocardial ischemia.

Acute myocardial infarction (AMI) continues to rank among the world's most leading causes of death and disability. Revascularization in a timely manner remains the most efficient method to save dying cardiomyocytes caused by AMI. Restoring blood flow to the ischemic region, however, results in further myocardial injury known as myocardial ischemia/reperfusion (MI/R) injury (Huang et al., 2024). Therefore, to maximize the advantages of myocardial revascularization during AMI, novel strategies for suppressing MI/R must be investigated.

Pharmacokinetics of small bioactive molecules as drugs can be influenced by interaction with plasma carrier proteins (Schmidt et al., 2010, Tang et al., 2013). Indeed, there has been much debate over the years regarding the impact of plasma protein binding on drug efficacy and, consequently, the therapeutic implications of variations in protein binding (Schmidt et al., 2010).

Alpha-2-macroglobulin ( $\alpha 2M$ ) with a homotetrameric quaternary structure (720 kDa) is known as an antiproteinase binding non-covalently to a variety of ligands (Ansari et al., 2023a,b). For this reason, the interaction of several bioactive small molecules such as gallic acid

\* Corresponding author at: Department of 28 Division of Cardiovascular, Beijing Anzhen Hospital, Capital Medical University, Beijing Institute of Heart, Lung and Blood Vessel Diseases, No. 2, Anzhen Road, Beijing 100029, China.

E-mail addresses: [magicdragon2001@163.com](mailto:magicdragon2001@163.com), [Jin-liu2@outlook.com](mailto:Jin-liu2@outlook.com) (J. Liu).

<https://doi.org/10.1016/j.arabjc.2024.106014>

Received 18 July 2024; Accepted 6 October 2024

Available online 9 October 2024

1878-5352/© 2024 The Authors. Published by Elsevier B.V. on behalf of King Saud University. This is an open access article under the CC BY-NC-ND license (<http://creativecommons.org/licenses/by-nc-nd/4.0/>).

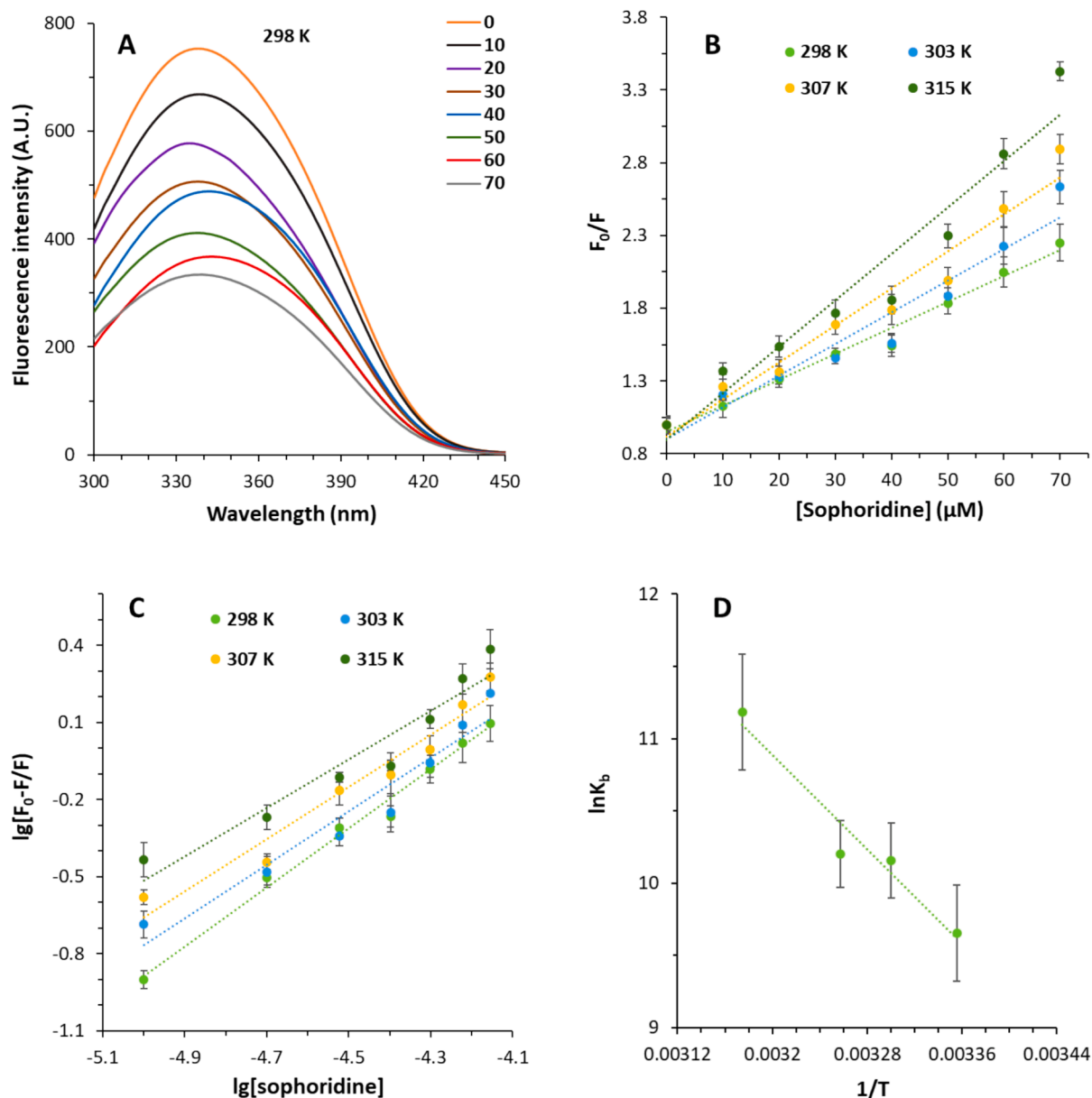


**Fig. 1.** (A) Interaction of  $\alpha 2M$  and sophoridine explored by fluorescence spectroscopy at room temperature. The  $\alpha 2M$  concentration was  $10 \mu M$  and added by increasing concentrations of sophoridine ( $10\text{--}70 \mu M$ ). (B) Stern-Volmer plots of the  $\alpha 2M$ -sophoridine complex at different temperatures. (C) Modified Stern-Volmer plots of the  $\alpha 2M$ -sophoridine complex at different temperatures. (D) van Hoff's plot of the  $\alpha 2M$ -sophoridine complex at different temperatures.

**Table 1**

Quenching parameters of the  $\alpha 2M$ -sophoridine complex explored by fluorescence spectroscopy measurement.

System	T (K)	$K_{SV} (M^{-1})$	$k_q (M^{-1} s^{-1})$	$R^2$
$\alpha 2M$ -sophoridine	298	$1.78 \times 10^4$	$1.78 \times 10^{12}$	0.9845
	303	$2.18 \times 10^4$	$2.18 \times 10^{12}$	0.9401
	307	$2.54 \times 10^4$	$2.54 \times 10^{12}$	0.9575
	315	$3.19 \times 10^4$	$3.19 \times 10^{12}$	0.9406

(Siddiqui et al., 2019), ferulic acid (Rehman et al., 2017), quercetin (Siddiqui et al., 2020), and morin (Ansari et al., 2023a,b) with  $\alpha 2M$  has been evaluated.

Thus, as the main objective of this work, we used a combination of molecular docking analysis and several spectroscopic techniques to investigate the interaction between sophoridine and  $\alpha 2M$ . Subsequently, using various cellular and molecular experiments, the protective effects

**Table 2**

Binding parameters of the  $\alpha 2M$ -sophoridine complex explored by fluorescence spectroscopy measurement.

System	T (K)	$lgK_b$	n	$R^2$
$\alpha 2M$ -sophoridine	298	4.19	9.42	0.9236
	303	4.41	1.01	0.9516
	307	4.43	1.04	0.9395
	315	4.86	1.49	0.9891

of  $\alpha 2M$  against MI/R injury in cardiomyocyte and the related signaling cascade were evaluated.

**Table 3**

Thermodynamic parameters of the  $\alpha_2$ M-sophoridine complex explored by fluorescence spectroscopy measurement.

System	T (K)	$\Delta H^0$ (kJ/mol)	$\Delta S^0$ (J/mol K <sup>-1</sup> )	$\Delta G^0$ (kJ/mol)
$\alpha_2$ M-sophoridine	298	67.67	306.851	-23.76
	303			-25.30
	307			-26.52
	315			-28.98

## 2. Materials and methods

### 2.1. Materials

Alpha-2-macroglobulin from human plasma ( $\geq 95\%$ , SDS-PAGE, Cat No: SRP6314), and 1-anilinoanthracene-8-sulfonate (ANS) were purchased from Sigma (USA). Sophoridine ( $\geq 98.0\%$ , Cat. No.: CS-0016780) from ChemScene LLC (USA). All other materials were of analytical grade and used without further purification.

### 2.2. Fluorescence spectroscopy

The fluorescence spectroscopy was done using a Shimadzu RF-5301 spectrophotometer (Tokyo, Japan). Intrinsic fluorescence spectroscopy measurements were carried out through exciting the  $\alpha_2$ M solution at a wavelength of 280 nm and reading the emission spectra at a wavelength range of 300–450 nm. The slit width for excitation and emission was set at 10 and 5 nm, respectively. The  $\alpha_2$ M concentration was fixed at 10  $\mu$ M. The protein sample was then incubated with increasing concentrations of sophoridine (10–70  $\mu$ M) for 2 min. Then the intrinsic fluorescence spectra were determined at four temperatures of 298, 303, 307, and 315 K. The intrinsic emission spectrum of sophoridine alone was also detected to exclude the interference of protein fluorescence signal by ligand. ANS fluorescence spectra were recorded to examine the effect of sophoridine on the surface hydrophobicity changes in  $\alpha_2$ M. The interaction of  $\alpha_2$ M/ANS (10/100  $\mu$ M) and sophoridine (70  $\mu$ M) was explored by ANS fluorescence spectroscopy at room temperature. The samples were excited at 360 nm and excitation was read in the range of 400–600 nm. All spectra were corrected against inner filter effect as previously described (El Gammal et al., 2022).

### 2.3. Far-UV circular dichroism (CD)

Far-UV CD spectra measurements were done using a JASCO J-1500 spectropolarimeter. CD spectra of  $\alpha_2$ M (20  $\mu$ M) and  $\alpha_2$ M-morin mixture (70  $\mu$ M) were recorded at room temperature. Each spectrum was recorded from the average of three scans with a scanning speed of 500 nm/min. All CD spectra were corrected against baseline spectra of buffer and ligand chirality.

### 2.4. Molecular docking

Molecular docking analysis of  $\alpha_2$ M with sophoridine was performed using AutoDock Vina software. The 3D crystal structures of  $\alpha_2$ M (PDB ID: 6TAV) and sophoridine (PubChem CID: 165549) were obtained from the RCSB Protein Data Bank and PubChem, respectively. AutoDock tools were used to perform the  $\alpha_2$ M and sophoridine preparation, which were removing bound ligand and water molecules, and adding Kollman charges and hydrogen atoms. To cover the  $\alpha_2$ M structure, the grid center was modified to X = 15.38, Y = 138.4, Z = 56.36 with a grid-box dimension of X = 82, Y = 126, Z = 126.

### 2.5. Cell culture

H9c2 cardiomyocyte cells obtained from the American Type Culture Collection (ATCC, USA.) were cultured in DMEM (Gibco, USA) containing 10 % fetal calf serum (FCS, Gibco, USA) in a humidified incubator with 5 % CO<sub>2</sub> at 37 °C. The medium was renewed every 2–3 days, and cells were used for experimental studies at 80–90 % confluence.

### 2.6. Myocardial ischemia/reperfusion (MI/R) injury model *in vitro*

To induce the MI/R injury *in vitro*, this experiment was done using the method previously established (Esumi et al., 1991) and reused in Yin et al. paper (Yin et al., 2013). Briefly, H9c2 cardiomyocyte cells were exposed to an ischemic buffer (Yin et al., 2013) in a hypoxic/ischemic chamber (Anaerocult® A mini, Merck) for 2 h in a humidified incubator with 5 % CO<sub>2</sub> and 95 % nitrogen at 37 °C. To perform reperfusion, the cells were cultured in fresh medium in the presence or absence of sophoridine (20  $\mu$ M) for 2 h at 95 % O<sub>2</sub> and 5 % CO<sub>2</sub>.

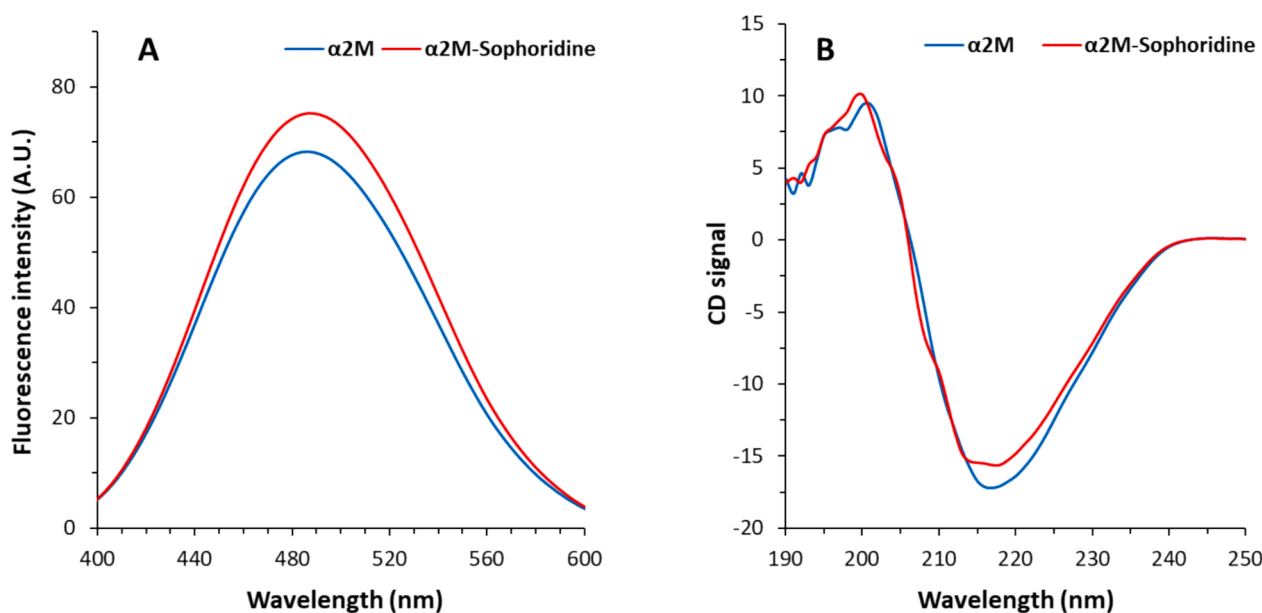


**Fig. 2.** (A) Interaction of  $\alpha_2$ M (10  $\mu$ M) and sophoridine (70  $\mu$ M) explored by ANS fluorescence spectroscopy at room temperature. (B) Interaction of  $\alpha_2$ M (20  $\mu$ M) and sophoridine (70  $\mu$ M) explored by Circular dichroism study.

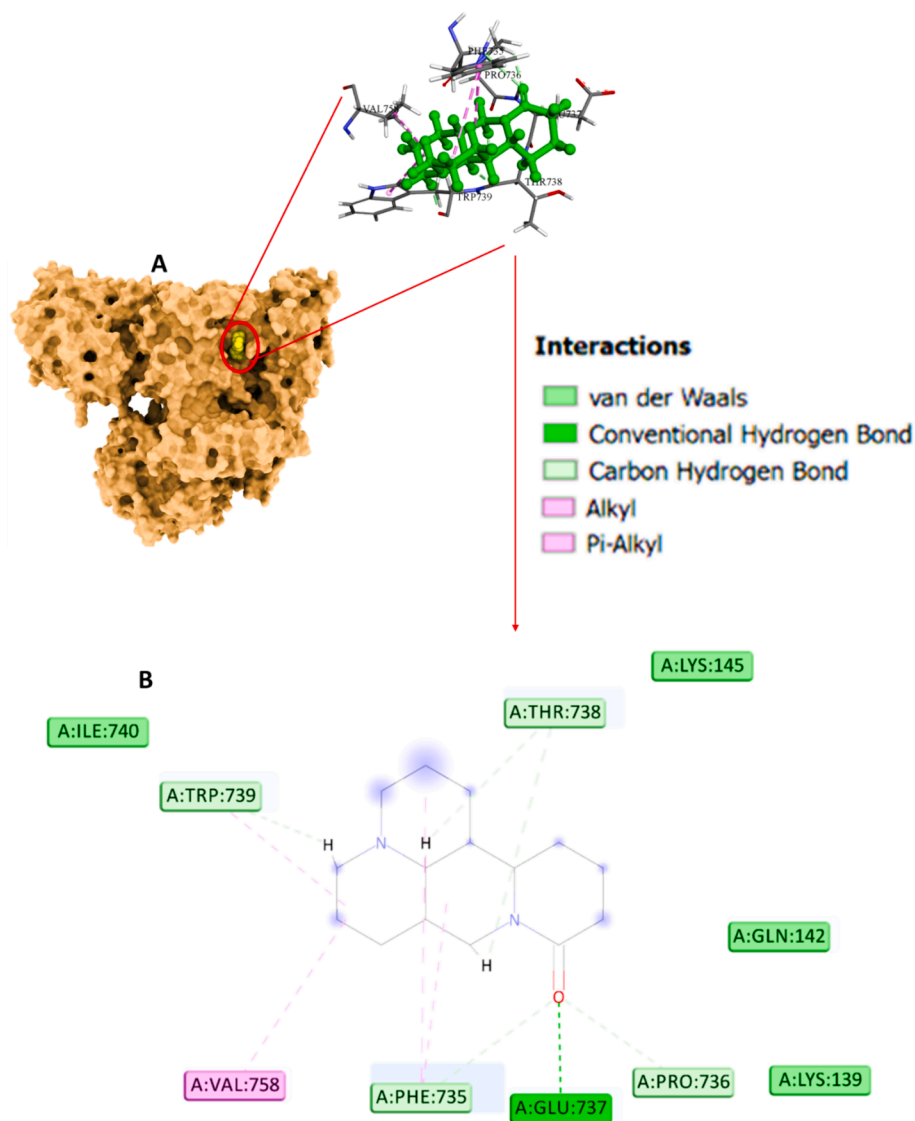


Fig. 3. (A) Interaction of  $\alpha$ 2M and sophoridine explored by molecular docking study. (B) Amino acid residues in the binding pocket.

Table 4

Specification of the  $\alpha$ 2M-sophoridine interaction explored by molecular docking study.

Amino acids	Distance	Type
GLU737	1.81	Conventional Hydrogen Bond
PHE735	3.05	Carbon Hydrogen Bond
PRO736	2.37	Carbon Hydrogen Bond
THR738	1.94	Carbon Hydrogen Bond
TRP739	1.75	Carbon Hydrogen Bond
VAL758	4.73	Alkyl
PHE735	4.82	Pi-Alkyl
PHE735	4.73	Pi-Alkyl
TRP739	4.90	Pi-Alkyl

### 2.7. Cell viability analysis

The vehicle and treated H9C2 cells were used for cell viability study using MTT assay (Yin et al., 2013). Briefly, 20  $\mu$ l of MTT solution (5 mg/ml) was added to each well ( $\times 10^4$  cells/well) followed by incubation for 4 h at 37  $^{\circ}$ C, aspiration of supernatants, and adding 150  $\mu$ l DMSO. After 15 min, the optical density was read at 490 nm using a Microplate Reader (Synergy-HT, BioTek, USA).

### 2.8. Measurement of lactate dehydrogenase (LDH) release

To membrane damage study was assessed using the Lactate Dehydrogenase Activity Assay Kit (MAK066, Sigma, USA). After experimental treatment, the culture medium of cells was removed and used for LDH activity according to the manufacturer's protocol at 450 nm on a Microplate Reader (Synergy-HT, BioTek, USA).

### 2.9. Measurement of reactive oxygen species (ROS)

Cells were washed with PBS and then incubated with 1 ml working solution of 2,7-dichlorofluorescein diacetate (DCFH-DA, Sigma, USA) at 37  $^{\circ}$ C for 30 min. Then, the cells were washed with PBS, lysed, and centrifuged at 2300g for 10 min (Ahamed et al., 2013). The fluorescence intensity of dichlorofluorescein (DCF) in the supernatant (200  $\mu$ l) was read at 485 nm excitation and 520 nm emission using a Microplate Reader (Synergy-HT, BioTek, USA).

### 2.10. Oxidative stress assay

The vehicle and treated H9C2 cells were used for oxidative stress assays using commercial Kits, malondialdehyde (MDA, cat. no. ab118970), and catalase (CAT, cat. no. ab83464) according to the

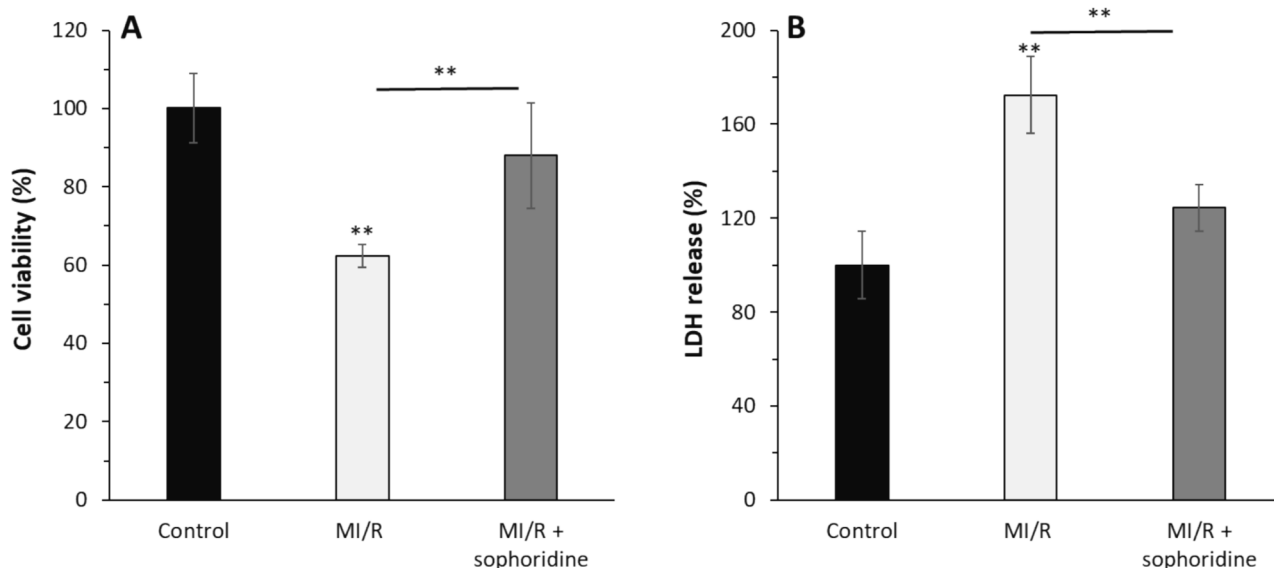


Fig. 4. After the induction of MI/R injury *in vitro*, the protective effects of sophoridine (20  $\mu$ M) for 2 h on cell viability and membrane leakage were assessed by (A) MTT assay and (B) LDH assay. \*\* $P < 0.01$ . The data are presented as mean  $\pm$  SD of three experiments.

manufacturer's protocol.

#### 2.11. Enzymatic caspase-9, -3 assay

The caspase activity was measured using the manufacturer's protocol (Promega Corporation, Madison, WI, USA) (Yin et al., 2013). Briefly, cells were harvested, washed, lysed, and centrifuged at 14,000 rpm for 15 min. Then, protein concentration was determined by Bradford Kit (Sigma, USA) and a fixed protein concentration was incubated with caspase assay buffer (30  $\mu$ l) as well as caspase substrates (2  $\mu$ l) at 37  $^{\circ}$ C for 4 h. The caspase activity was measured at 405 nm on a Microplate Reader (Synergy-HT, BioTek, USA).

#### 2.12. Quantitative real-time PCR (qPCR)

All cells were washed with PBS several times and then RNeasy Mini Kit (Qiagen, Hilden, Germany) was used to extract RNA following the manufacturer's protocol. Then, cDNA was synthesized by reverse transcription reaction with QuantiTect Reverse Transcription Kit (TaKaRa, Dalian, China). DNA was amplified with selective primers (Bax, Bcl-2, caspase-9, caspase-3) and the internal control gene (GAPDH) (Fang et al., 2018). SyberGreen qPCR Mix (TaKaRa, Dalian, China) was used for qPCR following the manufacturer's protocol. Real-Time PCR experiment was done using an ABI-step I plus (Applied Biosystems, Foster City, CA, USA) instrument. The relative expression was done through standardization of the expression of target genes by GAPDH and expressed as fold change using the  $2^{-\Delta\Delta C_t}$  method.

#### 2.13. ELISA analysis

After treatment, the cells were collected, lysed, and centrifuged at 4  $^{\circ}$ C for 20 min at 10,000 rpm (Yin et al., 2013). After the determination of protein concentration by Bradford assay, 30  $\mu$ g of protein was used for the assessment of human phosphorylated type of PI3K (p-PI3K, ELISA Kit, Cat. No: MBS167579, MyBioSource, Inc. USA) and p-Akt (ELISA Kit Cat. No: MBS9518725, MyBioSource, Inc. USA) following the manufacturer's protocol.

#### 2.14. Statistical analysis

SPSS was used to perform statistical analysis. Data were reported as

the mean  $\pm$  standard deviation (SD) of three experiments. The statistical comparisons were done with an analysis of variance (ANOVA) followed by a post hoc Tukey's test.  $P < 0.05$  was considered to show a statistically significant difference.

### 3. Results and discussion

#### 3.1. Fluorescence quenching study

The intrinsic fluorescence signal of  $\alpha$ 2M was measured and then compared to the fluorescence spectra of the  $\alpha$ 2M-sophoridine complexes to measure structural changes of proteins induced by the ligand (Rehman et al., 2017). The effect of ligand (sophoridine) on  $\alpha$ 2M intrinsic fluorescence intensity is exhibited in Fig. 1A. The addition of sophoridine to  $\alpha$ 2M led to a decrease in the intrinsic fluorescence signal of  $\alpha$ 2M evidenced by fluorescence spectra. This finding infers the probable microenvironmental changes around the  $\alpha$ 2M chromophore (Zia et al., 2024). Also, as shown in Fig. 1A, the maximum wavelength of  $\alpha$ 2M was red-shifted from around 340–335 nm upon interaction with 70  $\mu$ M sophoridine. This small red shift in maximum emission wavelength corroborates with the possible conformational changes around chromophores, Trp and Tyr residues (Zia et al., 2019; Siddiqui et al., 2020).

#### 3.2. Fluorescence quenching mechanism

The fluorescence quenching mechanism could be categorized as dynamic, static, or both static-dynamic for the interaction of a ligand-protein (Katrachali et al., 2023; Rehman et al., 2024; Shamsi et al., 2024). Dynamic and static-type quenching refers to collisions and ground-state complex formation between the receptor and quencher, respectively (Agrawal et al., 2019; Rehman et al., 2024). By analyzing fluorescence quenching data, the probable type of fluorescence quenching mechanism can be determined using Stern–Volmer Eq. (1) as follows (Rehman et al., 2024):

$$F_0/F = 1 + K_{SV}[\text{sophoridine}] = 1 + k_q\tau_0[\text{sophoridine}] \quad (1)$$

where  $F_0$  is the fluorescence intensity of the free  $\alpha$ 2M,  $F$  is the fluorescence intensity of the  $\alpha$ 2M-sophoridine,  $K_{SV}$  is the Stern–Volmer quenching constant,  $k_q$  is the bimolecular rate constant, and  $\tau_0$  is the Trp fluorescence average life-time ( $10^{-8}$  s) (Ansari et al., 2023a,b). Based on a plot of  $F_0/F$  against [sophoridine] with linear regression, the

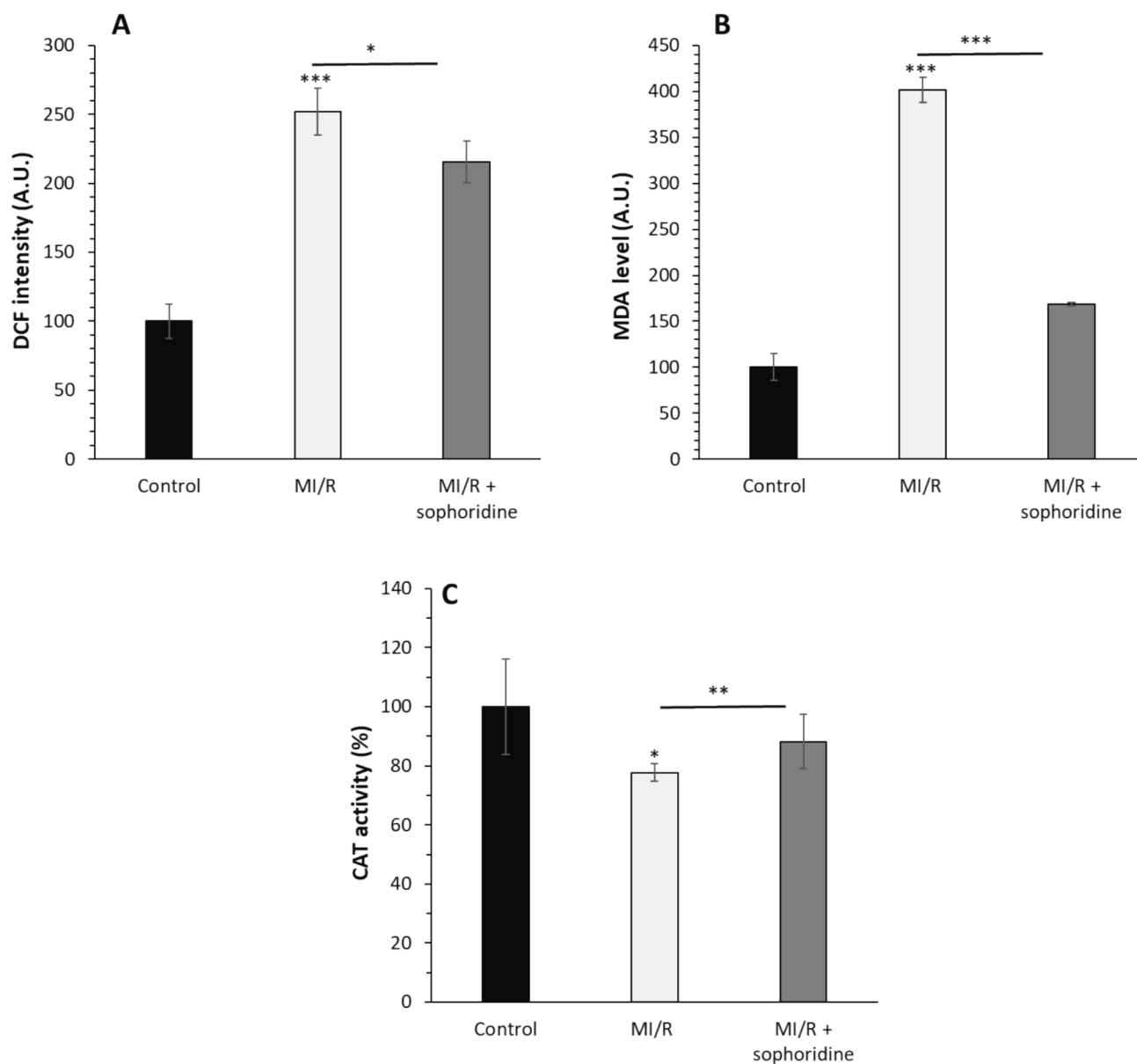


Fig. 5. After the induction of MI/R injury *in vitro*, the protective effects of sophoridine (20  $\mu\text{M}$ ) for 2 h on oxidative stress were assessed by (A) ROS assay, (B) MDA level, (C) CAT activity assay. \* $P < 0.05$ , \*\* $P < 0.01$ , \*\*\* $P < 0.001$ . The data are presented as mean  $\pm$  SD of three experiments.

fluorescence quenching constants can be determined (Fig. 1B).  $K_{SV}$  and  $k_q$  values are determined and then listed in Table 1.

It can be seen that there is a direct relationship between  $K_{SV}$  values and temperature, revealing that the fluorescence quenching type of  $\alpha 2\text{M}$  by sophoridine occurs through a dynamic mechanism (Bekhouché et al., 2012). However, the  $k_q$  values for the fluorescence quenching of  $\alpha 2\text{M}$  by sophoridine exceeds the threshold of biomolecule's limiting diffusion constant ( $2.0 \times 10^{10} \text{ dm}^3 \text{ mol}^{-1} \text{ s}^{-1}$ ), supporting the existence of a static mechanism (Manivel et al., 2023). Therefore, it can be claimed that both static-dynamic mechanisms mediate the decrease in fluorescence intensity of  $\alpha 2\text{M}$  by sophoridine.

### 3.3. Binding affinity

If every ligand independently interacts with a binding site on a protein, the binding affinity for a protein–ligand system can be calculated using Eq. (2) given below [28]:

$$\lg(F_0 - F/F) = \lg K_b + n \lg[\text{sophoridine}] \quad (2)$$

where  $n$  and  $K_b$  are the number of binding sites and the binding constant, respectively. The other parameters are the same as Eq. (1). By plotting  $\lg(F_0 - F/F)$  vs  $\lg[\text{sophoridine}]$ , straight lines were used to calculate  $\lg K_b$  and  $n$  values (Fig. 1C, Table 2).

One binding site was determined for sophoridine on  $\alpha 2\text{M}$  evidenced by  $n$  values, which are around 1. Upon increasing temperature, the  $n$  values decrease, likely due to the change in the population of ligand molecules in the ground state at higher temperatures (Gokavi et al., 2023). The calculated  $K_b$  values were around  $10^4$ , demonstrating a favorable (moderate) interaction between sophoridine and  $\alpha 2\text{M}$ . It was also found that the  $K_b$  values are higher in 315 K compared to 298 K, revealing the greater stability of the  $\alpha 2\text{M}$ -sophoridine complex at higher temperatures stemmed from the involvement of hydrophobic, hydrogen bonding, and electrostatic interactions, which will be further studied in the next section.

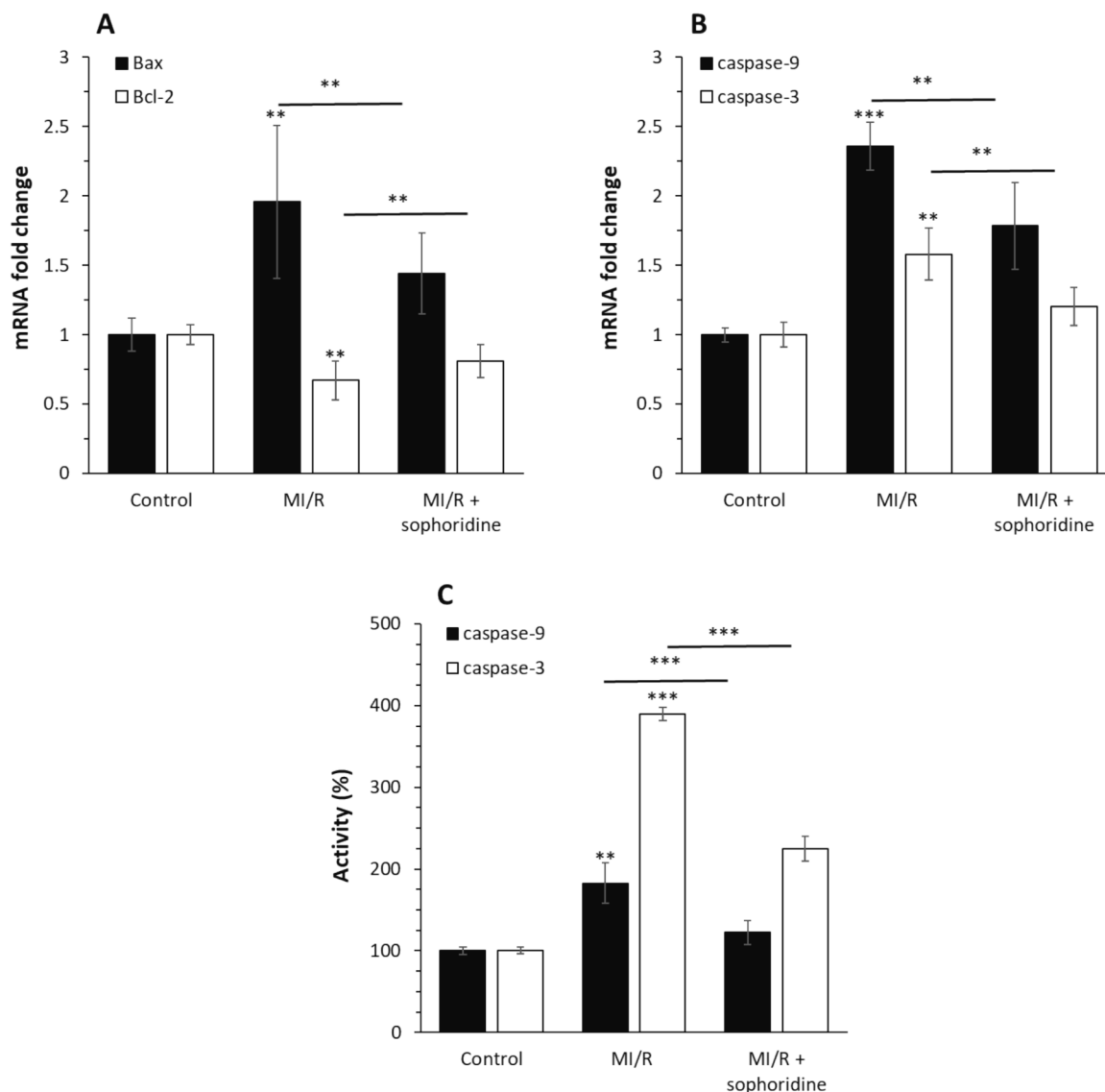


**Fig. 6.** After the induction of MI/R injury *in vitro*, the protective effects of sophoridine (20  $\mu$ M) for 2 h against apoptosis were assessed by (A) qPCR assay for expression of Bax and Bcl-2 genes, (B) qPCR assay for expression of caspase-9 and caspase-3 genes, (C) caspase-9 and caspase-3 activity assay. \*\* $P < 0.01$ , \*\*\* $P < 0.001$ . The data are presented as mean  $\pm$  SD of three experiments.

### 3.4. Thermodynamic analysis

The potential forces involved in the interaction of sophoridine and  $\alpha$ 2M could be determined from the values of enthalpy change ( $\Delta H^0$ ) and entropy change ( $\Delta S^0$ ) which can be determined using van Hoff's Eq. (3) as follows (Gokavi et al., 2023):

$$\ln K_b = \Delta H^0 / RT + \Delta S^0 / R \quad (3)$$

$R$ ,  $K_b$  and  $T$  are the universal gas constant, binding constant, and temperature, respectively. The  $\Delta H^0$  and  $\Delta S^0$  upon the quenching process can be determined by the slope and the intercept of  $\ln K_b$  against  $1/T$  plot (Fig. 1D), respectively.

Then, as demonstrated in Eq. (4), the free energy change ( $\Delta G^0$ ) can be calculated by the Gibbs-Helmholtz relationship (Gokavi et al., 2023):

$$\Delta G^0 = \Delta H^0 - T\Delta S^0 \quad (4)$$

According to Table 3,  $\Delta H^0$  and  $\Delta S^0$  values were 67.67 kJ mol<sup>-1</sup> and 306.851 J mol<sup>-1</sup> K<sup>-1</sup>, respectively. Therefore, it was deduced that the formation of the  $\alpha$ 2M-sophoridine complex was based on an enthalpy-

unfavorable but entropy-favorable, according to the thermodynamic outcome. This system shows that the binding of  $\alpha$ 2M to sophoridine was endothermic and entropy-driven (Fatima et al., 2017). This finding suggested that hydrophobic forces play a key part in the interaction between  $\alpha$ 2M and sophoridine, although the contribution of other hydrophilic forces should not be neglected (Fatima et al., 2017). Also, the negative values of  $\Delta G^0$  reveal that the binding of  $\alpha$ 2M and sophoridine is a spontaneous-driven process (Mohammadi et al., 2024).

### 3.5. Structural changes studies

Results from ANS fluorescence spectroscopy measurement provided detailed information for the interaction of sophoridine and  $\alpha$ 2M. The surface hydrophobicity of the protein is the most frequently marker employed in research on protein conformational changes (Alizadeh-Pasdar and Li-Chan 2000, Wang et al., 2024). Because of its strong affinity for interacting with nonpolar residues, the ANS fluorescence intensity measurement offers detailed insight for examining the exposure of some hydrophobic protein patches (Wang et al., 2024). The measured ANS fluorescence intensity is heavily dependent on the hydrophobic

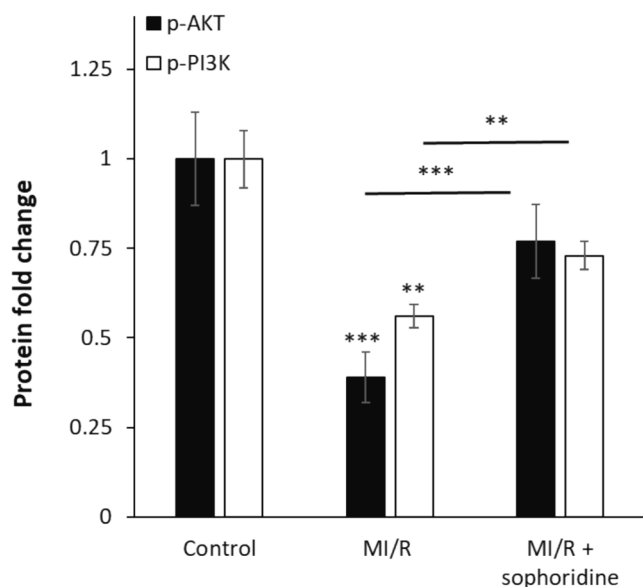


Fig. 7. After the induction of MI/R injury *in vitro*, the protective effects of sophoridine (20  $\mu$ M) for 2 h on the regulation of AKT/PI3K signaling pathways were assessed by ELISA. \*\* $P < 0.01$ , \*\*\* $P < 0.001$ . The data are presented as mean  $\pm$  SD of three experiments.

properties of a protein (Li et al., 2024). The ANS fluorescence spectra of  $\alpha_2$ M in the presence and absence of sophoridine were recorded and displayed in Fig. 2A. The ANS fluorescence spectrum of  $\alpha_2$ M was detected to slightly increase at 484 nm upon interaction with 70  $\mu$ M of sophoridine, suggesting the partial exposure of hydrophobic residues (Li et al., 2024). As a result, the conformational changes of  $\alpha_2$ M through exposure of some hydrophobic groups caused by interaction with sophoridine.

The interaction of small molecules with proteins could also induce significant structural changes in proteins (Ansari et al., 2023a,b). Indeed, the secondary structure of protein is a crucial aspect of protein stability and relevant function (Zeeshan et al., 2019). The changes in the protein secondary conformer upon ligand binding is typically analyzed using far-UV CD spectrum (190–250 nm) (Sreerama et al., 2000). The far-UV CD spectrum of free  $\alpha_2$ M depicts a minimum at 217 nm (Fig. 2D), which is characteristics of the dominance of  $\beta$ -sheet structure (Ansari et al., 2023a,b; Ansari et al., 2024). Upon the presence of sophoridine, the intensity (chirality) of the minimum (217 nm) slightly reduced (Fig. 2D), suggesting the partial changes in the secondary structure of  $\alpha_2$ M (Ansari et al., 2024). In other words, following incubation with sophoridine, no significant far-UV CD peak shifting or changes were observed, which indicated a partial decrease in  $\beta$ -sheet structure content of  $\alpha_2$ M (Zia et al., 2022; Ansari et al., 2023a,b).

### 3.6. Molecular docking study

Molecular docking as a theoretical approach is widely used to study the interactions between ligands and proteins. By this method, we can obtain detailed information about the location of the ligands in the protein binding site (Fu et al., 2018). Based on the unique structure adopted by proteins in the biological media, a small molecule can bind to different proteins in various modes depending on the hydrogen bond pairing and surface shape complementarity (Luo et al., 2010). In the present study, in the docking analysis, the energetically most favorable docked site of sophoridine and  $\alpha_2$ M with a binding score of  $-6.93$  kcal mol $^{-1}$  is shown in Fig. 3A. Further analysis indicated that sophoridine exhibits several hydrophobic and hydrogen bond interactions with  $\alpha_2$ M (Fig. 3B, Table 4). The binding site analysis demonstrated hydrogen bonding interaction between sophoridine and  $\alpha_2$ M amino acid residues

at the sites of GLU737, PHE735, PRO736, THR738, TRP739 (Fig. 3B). Moreover, sophoridine interacted with VAL758, PHE735, PHE735, and TRP739 amino acid residues through hydrophobic forces (Alkyl, Pi-Alkyl, Pi-Alkyl, Pi-Alkyl) (Fig. 3B).

Experimental data showed that the interaction of sophoridine with  $\alpha_2$ M led to fluorescence quenching. A molecular docking study reveals that TRP739 amino acid residue is placed in the docked pose of the  $\alpha_2$ M-sophoridine complex. Hence, the finding of the molecular docking study in agreement with experimental data imply that  $\alpha_2$ M molecule has a favorable affinity for sophoridine, and hydrophobic interactions and hydrogen bonds are the most contributing forces in the complexation process.

### 3.7. Sophoridine protects cardiomyocytes against MI/R injury *in vitro*

H9c2 cardiomyocyte viability after MI/R was studied by MTT assay (Fig. 4A). When compared to the control cells, it was shown that MI/R significantly reduced cardiomyocyte cell viability to  $62.32 \pm 2.94$  % (\*\* $P < 0.01$ ), however sophoridine therapy (20  $\mu$ M) significantly increased cell viability to  $87.97 \pm 13.57$  %. This data pointed out that cell survival was considerably restored by the treatment of cells with sophoridine.

Furthermore, cytoplasmic enzyme amount in cell culture medium as a marker of cell membrane damage showed that LDH release notably increased to  $172.39 \pm 16.31$  % after MI/R compared to the control group ( $P < 0.01$ ) (Fig. 4B). However, sophoridine treatment led to a decrease in LDH release to  $124.42 \pm 9.84$  % ( $P < 0.01$ ) at the end of reperfusion. This data is in good agreement with previous studies indicating that several kinds of naturally occurring compounds such as coptisine (Wang et al., 2017), matrine (Guo et al., 2018), oxymatrine (Zhang et al., 2021), and sinomenine (Xia et al., 2022) could confer protection against MI/R injury by mitigation of membrane damage.

### 3.8. Sophoridine protected cardiomyocytes from oxidative stress

Numerous studies have shown that regulating oxidative stress is a potential strategy that bioactive materials can trigger their protective effects against MI/R injury (Yu et al., 2016; Shu et al., 2019; He et al., 2024). Therefore, in this study, we aimed to assess the oxidative stress markers such as ROS, MDA and CAT in H9C2 cells. The data showed that the ROS (Fig. 5A) and MDA (Fig. 5A) levels were remarkably elevated by MI/R injury; however, these contents were reduced following treatment with sophoridine. The CAT activity in cardiomyocytes subjected to MI/R injury was significantly inhibited relative to the control group (Fig. 5C). However, sophoridine notably recovered the CAT activity in MI/R-triggered H9C2 cardiomyocytes (Fig. 5C).

Xia et al. reported that sinomenine as an alkaloid obtained from *Sinomenium acutum* could show protective effects against MI/R injury by mitigation of oxidative stress-mediated by inhibition of ROS generation and MDA formation (Xia et al., 2022). Therefore as mechanistic insight, it can be suggested that alkaloids could modulate the cardiomyocyte cytotoxicity stemming from MI/R injury through attenuating oxidative stress via upregulation of antioxidant enzymes as well as reduction of ROS and MDA formation (Qi et al., 2024).

### 3.9. Sophoridine protected cardiomyocytes from apoptosis

The intrinsic pathway of apoptosis is hardly regulated by mitochondria mediated by the regulation of the Bcl-2 family (Dadsena et al., 2021; Wolf et al., 2022). While Bcl-2 acts as an anti-apoptotic effector, Bax is a pro-apoptotic marker (Czabotar and Garcia-Saez 2023). Upregulation of Bcl-2 and downregulation of Bax have been previously shown to promote the anti-apoptotic effects of bioactive compounds in cardiomyocytes against MI/R injury (Yu et al., 2016; Su et al., 2022; Ge et al., 2023). Also, mitochondrial apoptosome-driven caspase upregulation has been known as an important mechanism triggered by

cytotoxic effects and leads to the activation of several caspases in apoptosis (Creagh et al., 2003). The activation of caspases-3 and -9, however, has been exhibited to serve as the most important stimulatory factor for the induction of apoptosis during MI/R injury (Stephanou et al., 2001). Therefore, protecting cardiomyocytes from MI/R injury could be mediated by blocking caspase-3 and caspase-9 expression and activity during apoptosis (Liu et al., 2020).

To explore how sophoridine protects cardiomyocytes against cytotoxicity induced by MI/R injury *in vitro*, apoptosis markers via the intrinsic pathway, expression of Bcl-2, Bax, caspase-9, and caspase-3 mRNA along with caspase-9 and caspase-3 activity assays in H9c2 cardiomyocyte cells were studied. As shown in Fig. 6A, B, MI/R significantly upregulated the relative mRNA level of pro-apoptotic proteins, Bax, caspase-9, and caspase-3, which was associated with the reduction of the anti-apoptotic protein, Bcl-2, relative to the control group. However, this mechanism was suppressed by incubation of cardiomyocytes with sophoridine. In addition, similar trends with caspase mRNA assays were observed in caspase activity studies (Fig. 6C).

These data revealed that sophoridine was able to inhibit the MI/R-initiated upregulation of apoptosis-associated genes, which is consistent with previous studies, describing the protective effects of natural compounds against MI/R injuries (Yin et al., 2013; Yu et al., 2016; Han et al., 2019). For example, Xing et al. reported that anisodamine as a natural alkaloid drug could show a potential cardioprotective effect against MI/R through regulation of apoptosis mediated by down-regulation of Bax/Bcl-2 protein ratio and expression of caspases (Xing et al., 2015).

### 3.10. Sophoridine activates PI3K/AKT signaling pathway

One important signaling cascade that regulates apoptosis is PI3K/AKT. The stimulation of the PI3K/AKT signaling pathway down-regulates the expression levels of caspase-3 and -9 (Ghafouri-Fard et al., 2022). Previous studies have mentioned that bioactive products are capable of inhibiting MI/R-stimulated cardiomyocyte apoptosis mediated by targeting PI3K/AKT (Syed Abd Halim et al., 2023). For example, Li et al. documented that piperine alkaloid, the primary component of the grains of black pepper, protects against MI/R injury mediated by upregulating the PI3K/AKT signaling pathway (Li et al., 2021). The same effects have been also reported for berberine which is able to attenuate MI/R injury via activation of the PI3K/AKT signaling pathway (Chen et al., 2014). Therefore, in this study, we assessed the activation of the PI3K/AKT signaling pathway in H9C2 cardiomyocytes exposed to MI/R in the absence and presence of sophoridine by ELISA assay. As shown in Fig. 7, MI/R markedly decreased the expression of p-PI3K and p-AKT in comparison with the control group. However, treatment of cells with sophoridine at the induction of MI/R upregulated the expression of p-PI3K and p-AKT compared with the MI/R-treated group.

Therefore, it can be surmised that MI/R injury was ameliorated by sophoridine, likely via activation of the PI3K/AKT signaling pathway. This data is consistent with previous studies, reporting the protective effects of bioactive compounds, particularly alkaloids, against MI/R injury via the upregulation of the PI3K/AKT signaling pathway (Chen et al., 2014; Li et al., 2021; Syed Abd Halim et al., 2023).

## 4. Conclusion

In conclusion, by using molecular docking and spectroscopic methods, it was found that  $\alpha$ 2M underwent partial structural changes upon hydrophobic interaction with sophoridine. The spontaneous and thermodynamically favorable formation of the  $\alpha$ 2M-sophoridine complex was evidenced by the negative value of  $\Delta G^0$  and positive values of  $\Delta H^0$  and  $\Delta S^0$ . The cellular assays showed that sophoridine had a potential protective effect in the cardiomyocytes against MI/R injury-induced apoptosis mediated by upregulation of the p-AKT/p-PI3K signaling pathway. Therefore, the favorable interaction of sophoridine

with plasma proteins and potential protective effects in cardiomyocytes will have an impact on the pathophysiology and etiology of MI/R injury. To address the limitation of this study, the potential application of sophoridine *in vivo* should be addressed to further discuss the pharmacokinetic and therapeutic properties of this small molecule as a drug.

## 5. Funding

No external funding was received.

## 6. Availability of data and materials

The datasets used and/or analyzed during the current study are available from the corresponding author on reasonable request.

## 7. Authors' contributions

All authors conceived and designed the experiments, performed the experiments, collected the data and finished the statistical analysis. All authors contributed to manuscript preparation and revision. All authors read and approved the final manuscript.

## 8. Ethics approval and consent to participate

Not applicable.

## 9. Patient consent for publication

Not applicable.

## CRediT authorship contribution statement

**Zheng Wu:** Writing – review & editing, Writing – original draft, Conceptualization, Methodology. **Shujuan Cheng:** Writing – review & editing, Writing – original draft, Conceptualization, Methodology. **Shaoping Wang:** Writing – review & editing, Writing – original draft, Conceptualization, Methodology. **Wenzheng Li:** Writing – review & editing, Writing – original draft, Conceptualization, Methodology. **Jinghua Liu:** Writing – review & editing, Writing – original draft, Conceptualization, Methodology, Supervision, Funding acquisition, Software.

## Declaration of competing interest

The authors declare that they have no known competing financial interests or personal relationships that could have appeared to influence the work reported in this paper.

## Acknowledgements

Not applicable.

## References

- Agrawal, R., Siddiqi, M.K., Thakur, Y., Tripathi, M., Asatkar, A.K., Khan, R.H., Pande, R., 2019. Explication of bovine serum albumin binding with naphthyl hydroxamic acids using a multispectroscopic and molecular docking approach along with its antioxidant activity. *Luminescence* 34 (6), 628–643.
- Ahamed, M., Ali, D., Alhadlaq, H.A., Akhtar, M.J., 2013. Nickel oxide nanoparticles exert cytotoxicity via oxidative stress and induce apoptotic response in human liver cells (HepG2). *Chemosphere* 93 (10), 2514–2522.
- Alagarsamy, V., Chitra, K., Saravanan, G., Solomon, V.R., Sulthana, M., Narendhar, B., 2018. An overview of quinazolines: Pharmacological significance and recent developments. *Eur. J. Med. Chem.* 151, 628–685.
- Alizadeh-Pasdar, N., Li-Chan, E.C., 2000. Comparison of protein surface hydrophobicity measured at various pH values using three different fluorescent probes. *J. Agric. Food Chem.* 48 (2), 328–334.

- Ansari, S., Ahsan, H., Zia, M.K., Gatasheh, M.K., Khan, F.H., 2023a. Exploring the interaction of myricetin with human alpha-2-macroglobulin: biophysical and in-silico analysis. *J. Biol. Phys.* 49 (1), 29–48.
- Ansari, S., Zia, M.K., Fatima, S., Ahsan, H., Khan, F.H., 2023b. Probing the binding of morin with alpha-2-macroglobulin using multi-spectroscopic and molecular docking approach: Interaction of morin with  $\alpha 2M$ . *J. Biol. Phys.* 49 (2), 235–255.
- Ansari, S., Arif, A., Zia, M.K., Ahsan, H., Ahmad, O., Khan, R.H., Khan, F.H., 2024. Investigation on the molecular interaction between dietary flavone luteolin and alpha-2-macroglobulin using multi-spectroscopic, calorimetric and molecular dynamics simulation techniques. *J. Mol. Liq.* 124198.
- Bekhouche, M., Blum, L.J., Doumèche, B., 2012. Contribution of dynamic and static quenchers for the study of protein conformation in ionic liquids by steady-state fluorescence spectroscopy. *J. Phys. Chem. B* 116 (1), 413–423.
- Chen, K., Li, G., Geng, F., Zhang, Z., Li, J., Yang, M., Dong, L., Gao, F., 2014. Berberine reduces ischemia/reperfusion-induced myocardial apoptosis via activating AMPK and PI3K–Akt signaling in diabetic rats. *Apoptosis* 19, 946–957.
- Chen, Y., Wang, X., Ye, D., Yang, Z., Shen, Q., Liu, X., Chen, C., Chen, X., 2023. Research progress of sophoridine's pharmacological activities and its molecular mechanism: an updated review. *Front. Pharmacol.* 14, 1126636.
- Creagh, E.M., Conroy, H., Martin, S.J., 2003. Caspase-activation pathways in apoptosis and immunity. *Immunol. Rev.* 193 (1), 10–21.
- Czabotar, P.E., Garcia-Saez, A.J., 2023. Mechanisms of BCL-2 family proteins in mitochondrial apoptosis. *Nat. Rev. Mol. Cell Biol.* 24 (10), 732–748.
- Dadsena, S., King, L.E., García-Sáez, A.J., 2021. Apoptosis regulation at the mitochondria membrane level. *Biochim. Biophys. Acta (BBA)-Biomembr.* 1863 (12), 183716.
- Dong, S., Zheng, X., Wang, Y., Xu, Y., 2022. An experimental study on anti-inflammatory and antioxidant effects of sophoridine in mice with lipopolysaccharide-induced acute lung injury. *Lat. Am. J. Pharm.* 41 (6), 1244–1248.
- El Gammal, R.N., Elmansi, H., El-Emam, A.A., Belal, F., Hammouda, M.E., 2022. Exploring the molecular interaction of mebendazole with bovine serum albumin using multi-spectroscopic approaches and molecular docking. *Sci. Rep.* 12 (1), 11582.
- Esumi, K., Nishida, M., Shaw, D., Smith, T.W., Marsh, J.D., 1991. NADH measurements in adult rat myocytes during simulated ischemia. *Am. J. Physiol. Heart Circulat. Physiol.* 260 (6), H1743–H1752.
- Fang, Z., Luo, W., Luo, Y., 2018. Protective effect of  $\alpha$ -mangostin against CoCl<sub>2</sub>-induced apoptosis by suppressing oxidative stress in H9c2 rat cardiomyoblasts. *Mol. Med. Rep.* 17 (5), 6697–6704.
- Fatima, S., Sen, P., Sneha, P., Priyadoss, C.G., 2017. Hydrophobic interaction between Domain I of Albumin and B Chain of detemir may support Myristate-dependent Detemir-Albumin binding. *Appl. Biochem. Biotechnol.* 182, 82–96.
- Fu, Y., Zhao, J., Chen, Z., 2018. Insights into the molecular mechanisms of protein-ligand interactions by molecular docking and molecular dynamics simulation: a case of oligopeptide binding protein. *Computat. Math. Methods Med.* 2018 (1), 3502514.
- Ge, F., Gao, X., Zhou, X., Li, J., Ma, X., Huang, M., Wuken, S., Tu, P., An, C., Chai, X., 2023. The alkaloids of *Corydalis hendersonii* Hems. contribute to the cardioprotective effect against ischemic injury in mice by attenuating cardiomyocyte apoptosis via p38 MAPK signaling pathway. *Chin. Med.* 18 (1), 29.
- Ghafari-Fard, S., Khanbabapour Sasi, A., Hussien, B.M., Shoorai, H., Siddiq, A., Taheri, M., Ayatollahi, S.A., 2022. Interplay between PI3K/AKT pathway and heart disorders. *Mol. Biol. Rep.* 49 (10), 9767–9781.
- Gokavi, N.M., Nandibewoor, S.T., Gowda, J.I., 2023. Investigations of the Interaction Mechanism Between Orphenadrine Hydrochloride and Bovine Serum Albumin by Spectroscopic and Voltammetric Techniques. *J. Fluoresc.* 33 (5), 2061–2073.
- Guo, S., Gao, C., Xiao, W., Zhang, J., Qu, Y., Li, J., Ye, F., 2018. Matrine protects cardiomyocytes from ischemia/reperfusion injury by regulating HSP70 expression via activation of the JAK2/STAT3 pathway. *Shock* 50 (6), 664–670.
- Han, X., Shi, H., Liu, K., Zhong, L., Wang, F., You, Q., 2019. Protective effect of gastrodin on myocardial ischemia-reperfusion injury and the expression of Bax and Bcl-2. *Exp. Ther. Med.* 17 (6), 4389–4394.
- He, J., Huang, L., Sun, K., Li, J., Han, S., Gao, X., Wang, Q.-Q., Yang, S., Sun, W., Gao, H., 2024. Oleuropein alleviates myocardial ischemia–reperfusion injury by suppressing oxidative stress and excessive autophagy via TLR4/MAPK signaling pathway. *Chin. Med.* 19 (1), 59.
- Huang, X., Bai, S., Luo, Y., 2024. Advances in research on biomarkers associated with acute myocardial infarction: a review. *Medicine* 103 (15), e37793.
- Katrahalli, U., Shanker, G., Pal, D., Hadagali, M.D., 2023. Molecular spectroscopic and docking analysis of the interaction of fluorescent thiacarbocyanine dye with biomolecule bovine serum albumin. *J. Biomol. Struct. Dyn.* 41 (20), 10702–10712.
- Li, Y.-P., Chen, Z., Cai, Y.-H., 2021. Piperine protects against myocardial ischemia/reperfusion injury by activating the PI3K/AKT signaling pathway. *Exp. Ther. Med.* 21 (4), 1–8.
- Li, D., Wang, S., Dong, J., Li, J., Wang, X., Liu, F., Ba, X., 2024. Inhibition and disaggregation effect of flavonoid-derived carbonized polymer dots on protein amyloid aggregation. *Colloids Surf. B Biointerfaces* 238, 113928.
- Liu, H., Li, S., Jiang, W., Li, Y., 2020. MiR-484 protects rat myocardial cells from ischemia-reperfusion injury by inhibiting caspase-3 and caspase-9 during apoptosis. *Kor. Circulat. J.* 50 (3), 250.
- Luo, W., Pei, J., Zhu, Y., 2010. A fast protein-ligand docking algorithm based on hydrogen bond matching and surface shape complementarity. *J. Mol. Model.* 16, 903–913.
- Macáková, K., Afonso, R., Saso, L., Mladěnka, P., 2019. The influence of alkaloids on oxidative stress and related signaling pathways. *Free Radic. Biol. Med.* 134, 429–444.
- Manivel, P., Marimuthu, P., Ilanchelian, M., 2023. Deciphering the binding site and mechanism of new methylene blue with serum albumins: a multispectroscopic and computational investigation. *Spectrochim. Acta A Mol. Biomol. Spectrosc.* 300, 122900.
- Mohammadi, M.A., Shareghi, B., Farhadian, S., Uversky, V.N., 2024. Investigating the effect of pH on the interaction of cypermethrin with human serum albumin: Insights from spectroscopic and molecular dynamics simulation studies. *Int. J. Biol. Macromol.* 257, 128459.
- Qi, J., Li, H., Yang, Y., Sun, X., Wang, J., Han, X., Chu, X., Sun, Z., Chu, L., 2024. Mechanistic insights into the ameliorative effects of hypoxia-induced myocardial injury by *Corydalis yanhusuo* total alkaloids: based on network pharmacology and experiment verification. *Front. Pharmacol.* 14, 1275558.
- Rehman, A.A., Sarwar, T., Arif, H., Ali, S.S., Ahsan, H., Tabish, M., Khan, F.H., 2017. Spectroscopic and thermodynamic studies on ferulic acid–alpha-2-macroglobulin interaction. *J. Mol. Struct.* 1144, 254–259.
- Rehman, A.A., Zaman, M., Arif, H., Ahsan, H., Khan, R.H., Khan, F.H., 2024. Interaction of esculetin with alpha-2-macroglobulin: biochemical and biophysical approaches. *J. Macromol. Sci. Part B* 1–13.
- Schmidt, S., Gonzalez, D., Derendorf, H., 2010. Significance of protein binding in pharmacokinetics and pharmacodynamics. *J. Pharm. Sci.* 99 (3), 1107–1122.
- Shamsi, A., Shahwan, M., Furkan, M., Khan, M.S., Yadav, D.K., Khan, R.H., 2024. Computational and spectroscopic insight into the binding of citral with human transferrin: targeting neurodegenerative diseases. *Heliyon* 10 (13).
- Shi, Q., Hui, S., Zhang, A.-H., Hong-Ying, X., Guang-Li, Y., Ying, H., Xi-Jun, W., 2014. Natural alkaloids: basic aspects, biological roles, and future perspectives. *Chin. J. Nat. Med.* 12 (6), 401–406.
- Shu, Z., Yang, Y., Yang, L., Jiang, H., Yu, X., Wang, Y., 2019. Cardioprotective effects of dihydroquercetin against ischemia reperfusion injury by inhibiting oxidative stress and endoplasmic reticulum stress-induced apoptosis via the PI3K/Akt pathway. *Food Funct.* 10 (1), 203–215.
- Siddiqui, T., Zia, M.K., Ali, S.S., Ahsan, H., Khan, F.H., 2019. Inactivation of alpha-2-macroglobulin by photo-illuminated gallic acid. *J. Fluoresc.* 29, 969–979.
- Siddiqui, T., Zia, M.K., Ahsan, H., Khan, F.H., 2020. Quercetin-induced inactivation and conformational alterations of alpha-2-macroglobulin: multi-spectroscopic and calorimetric study. *J. Biomol. Struct. Dyn.* 38 (14), 4107–4118.
- Song, T., Hao, Y., Wang, M., Li, T., Zhao, C., Li, J., Hou, Y., 2023. Sophoridine manifests as a leading compound for anti-arrhythmia with multiple ion-channel blocking effects. *Phytomedicine* 112, 154688.
- Sreerama, N., Venyaminov, S.Y., Woody, R.W., 2000. Estimation of protein secondary structure from circular dichroism spectra: inclusion of denatured proteins with native proteins in the analysis. *Anal. Biochem.* 287 (2), 243–251.
- Stephanou, A., Brar, B., Liao, Z., Scarabelli, T., Knight, R.A., Latchman, D.S., 2001. Distinct initiator caspases are required for the induction of apoptosis in cardiac myocytes during ischaemia versus reperfusion injury. *Cell Death Differ.* 8 (4), 434–435.
- Su, X., Zhou, M., Li, Y., An, N., Yang, F., Zhang, G., Xu, L., Chen, H., Wu, H., Xing, Y., 2022. Mitochondrial damage in myocardial Ischemia/Reperfusion injury and application of natural plant products. *Oxid. Med. Cell. Longev.* 2022 (1), 8726564.
- Syed Abd Halim, S.A., Abd Rashid, N., Woon, C.K., Abdul Jalil, N.A., 2023. Natural products targeting PI3K/AKT in myocardial ischemic reperfusion injury: A scoping review. *Pharmaceuticals* 16 (5), 739.
- Tang, Q., Liu, Y., Peng, X., Wang, B., Luan, F., Zeng, N., 2023. Research progress in the pharmacological activities, toxicities, and pharmacokinetics of sophoridine and its derivatives. *Drug Design Development and Therapy* 191–212.
- Tang, Y., Zhang, S., Lu, Y., Zhu, X., 2013. Analysis of plasma protein binding of sophoridine by ultrafiltration and high-performance liquid chromatography. *Lat Am J Pharm* 32, 139–142.
- ur Rashid, H., Rasool, S., Ali, Y., Khan, K., Martines, M.A.U., 2020. Anti-cancer potential of sophoridine and its derivatives: Recent progress and future perspectives. *Bioorg. Chem.* 99, 103863.
- Wang, Q., Li, Y., Li, K.-W., Zhou, C.-Z., 2022. Sophoridine: a review of its pharmacology, pharmacokinetics and toxicity. *Phytomedicine* 95, 153756.
- Wang, Y., Wang, Q., Zhang, L.U., Ke, Z., Zhao, Y., Wang, D., Chen, H., Jiang, X., Gu, M., Fan, S., 2017. Coptisine protects cardiomyocyte against hypoxia/reoxygenation-induced damage via inhibition of autophagy. *Biochem. Biophys. Res. Commun.* 490 (2), 231–238.
- Wang, N., Wang, X., Zhang, S., Wang, T., Yu, D., 2024. Non-covalent interaction between soybean protein isolate and naringenin: focused on binding mechanism, interface behavior, and functional properties. *Food Hydrocoll.* 153, 109975.
- Wolf, P., Schoeniger, A., Edlich, F., 2022. Pro-apoptotic complexes of BAX and BAK on the outer mitochondrial membrane. *Biochimica et Biophysica Acta (BBA)-Molecular. Cell Res.* 1869 (10), 119317.
- Xia, B., Li, Q., Wu, J., Yuan, X., Wang, F., Lu, X., Huang, C., Zheng, K., Yang, R., Yin, L., 2022. Sinomenine confers protection against myocardial ischemia reperfusion injury by preventing oxidative stress, cellular apoptosis, and inflammation. *Front. Pharmacol.* 13, 922484.
- Xing, K., Fu, X., Jiang, L., Wang, Y., Li, W., Gu, X., Hao, G., Miao, Q., Ge, X., Peng, Y., 2015. Cardioprotective effect of anisodamine against myocardial ischemia injury and its influence on cardiomyocytes apoptosis. *Cell Biochem. Biophys.* 73, 707–716.
- Yin, Y., Guan, Y., Duan, J., Wei, G., Zhu, Y., Quan, W., Guo, C., Zhou, D., Wang, Y., Xi, M., 2013. Cardioprotective effect of Danshensu against myocardial ischemia/reperfusion injury and inhibits apoptosis of H9c2 cardiomyocytes via Akt and ERK1/2 phosphorylation. *Eur. J. Pharmacol.* 699 (1–3), 219–226.
- Yu, Y., Sun, G., Luo, Y., Wang, M., Chen, R., Zhang, J., Ai, Q., Xing, N., Sun, X., 2016. Cardioprotective effects of Notoginsenoside R1 against ischemia/reperfusion injuries by regulating oxidative stress-and endoplasmic reticulum stress-related signaling pathways. *Sci. Rep.* 6 (1), 21730.

- Zeeshan, F., Tabbassum, M., Kesharwani, P., 2019. Investigation on secondary structure alterations of protein drugs as an indicator of their biological activity upon thermal exposure. *Protein J.* 38, 551–564.
- Zhang, Z., Qin, X., Wang, Z., Li, Y., Chen, F., Chen, R., Li, C., Zhang, W., Zhang, M., 2021. Oxymatine pretreatment protects H9c2 cardiomyocytes from hypoxia/reoxygenation injury by modulating the PI3K/Akt pathway. *Exp. Ther. Med.* 21 (6), 1–12.
- Zia, M.K., Siddiqui, T., Ali, S.S., Ahsan, H., Khan, F.H., 2019. Understanding the binding interaction between methotrexate and human alpha-2-macroglobulin: multi-spectroscopic and computational investigation. *Arch. Biochem. Biophys.* 675, 108118.
- Zia, M.K., Siddiqui, T., Ahsan, H., Khan, F.H., 2022. Comprehensive insight into the molecular interaction of an anticancer drug-ifosfamide with human alpha-2-macroglobulin: biophysical and in silico studies. *J. Biomol. Struct. Dyn.* 40 (9), 3907–3916.
- Zia, M.K., Siddiqui, T., Ansari, S., Muaz, M., Ahsan, H., Khan, F.H., 2024. Insight into the molecular interaction between the anticancer drug, enzalutamide and human alpha-2-macroglobulin: Biochemical and biophysical approach. *Spectrochim. Acta A Mol. Biomol. Spectrosc.* 311, 123957.